Molecular Cell *23*, 133–142, July 7, 2006 ©2006 Elsevier Inc. DOI 10.1016/j.molcel.2006.06.005

The Exonuclease TREX1 Is in the SET Complex and Acts in Concert with NM23-H1 to Degrade DNA during Granzyme A-Mediated Cell Death

Dipanjan Chowdhury,[1] Paul J. Beresford,[1] Pengcheng Zhu,[1] Dong Zhang,[1] Jung-Suk Sung,[3,4] Bruce Demple,[3] Fred W. Perrino,[2] and Judy Lieberman[1,*]

[1] CBR Institute for Biomedical Research
Department of Pediatrics
Harvard Medical School
Boston, Massachusetts 02115

[2] Department of Biochemistry
Wake Forest University School of Medicine
Winston-Salem, North Carolina 27157

[3] Department of Genetics and Complex Diseases
Harvard School of Public Health
Boston, Massachusetts 02115

Summary

Granzyme A (GzmA) activates a caspase-independent cell death pathway with morphological features of apoptosis. Single-stranded DNA damage is initiated when the endonuclease NM23-H1 becomes activated to nick DNA after granzyme A cleaves its inhibitor, SET. SET and NM23-H1 reside in an endoplasmic reticulum-associated complex (the SET complex) that translocates to the nucleus in response to superoxide generation by granzyme A. We now find the 3′-to-5′ exonuclease TREX1, but not its close homolog TREX2, in the SET complex. TREX1 binds to SET and colocalizes and translocates with the SET complex. NM23-H1 and TREX1 work in concert to degrade DNA. Silencing *NM23-H1* or *TREX1* inhibits DNA damage and death of cells treated with perforin (PFN) and granzyme A, but not of cells treated with perforin and granzyme B (GzmB). After granzyme A activates NM23-H1 to make single-stranded nicks, TREX1 removes nucleotides from the nicked 3′ end to reduce the possibility of repair by rejoining the nicked ends.

Introduction

Granzyme A (GzmA), an abundant serine protease in the cytolytic granules of cytolytic T cells and NK cells, activates caspase-independent cell death when it is delivered by perforin (PFN) into the target cell through the immunological synapse (Griffiths, 2003; Lieberman, 2003). GzmA does not activate the caspases or induce cleavage of most key caspase pathway substrates, such as bid or ICAD, and is able to kill target cells resistant to caspase-mediated cell death, including cells that overexpress *bcl-2* (Beresford et al., 1999; Martinvalet et al., 2005). This may be important for immune defense against cancers and viruses that have evolved strategies for evading caspase-mediated apoptosis. Target cells have all the morphological features of apoptosis. Chromatin condensation and nuclear fragmentation can be readily seen within a few hours (Beresford et al., 1999; Lieberman and Fan, 2003; Zhang et al., 2001a). A key feature of GzmA-mediated cell death is the initiation of single-stranded DNA damage, rather than the blunt double-stranded breaks characteristic of the caspase-activated DNase CAD (Beresford et al., 1999; Fan et al., 2003a; Shresta et al., 1999). These nicks produce multikilobase DNA fragments, which are not detected by assays that measure apoptotic DNA damage by production and release of short oligonucleosomal DNA fragments. However, GzmA-induced DNA damage can be detected by radiolabeling free single-stranded ends with TUNEL or the Klenow fragment of DNA polymerase or by separating the two strands of nicked chromosomal DNA using alkaline gel electrophoresis (Beresford et al., 1999, 2001; Fan et al., 2003a; Zhu et al., 2006).

DNA damage by GzmA is mediated by the 270–420 kDa SET complex (Beresford et al., 2001). Not all the components of this complex are known. The SET complex is mobilized during the cellular response to oxidative damage and is postulated to participate in the oxidative stress response (Martinvalet et al., 2005). When GzmA is delivered into a target cell, mitochondria are damaged to generate superoxide, and the SET complex, normally associated with the endoplasmic reticulum, translocates to the nucleus (Martinvalet et al., 2005). The SET complex contains both the endonuclease that makes the characteristic single-stranded cuts in GzmA-treated cells as well as a specific inhibitor of the nuclease. The GzmA-activated endonuclease is NM23-H1, which is also a tumor metastasis suppressor and nucleoside diphosphate kinase. Its inhibitor is the nucleosome assembly protein and GzmA substrate, SET (Fan et al., 2003a). When GzmA cuts SET, the NM23-H1 endonuclease is activated. The importance of NM23-H1 and SET in GzmA-mediated cell death was confirmed by finding increased DNA damage and cell death in cells that overexpress *NM23-H1* or have silenced *SET* and, conversely, by finding less cell death in targets with silenced *NM23-H1* or enhanced *SET* expression (Fan et al., 2003a). The SET complex also contains 2 additional GzmA substrates—the apurinic endonuclease responsible for base excision repair, Ape1 (Fan et al., 2003b), and the DNA-binding protein HMG-2 (Fan et al., 2002). pp32, a tumor suppressor protein that inhibits protein phosphatase PP2A, is also a component of the SET complex (Beresford et al., 2001).

Following GzmA treatment, the purified SET complex shows significant exonuclease activity on supercoiled plasmid DNA (Beresford et al., 2001; Fan et al., 2003a). Although NM23-H1 may have some 3′-to-5′ exonuclease activity, this activity has only been demonstrated on single-stranded DNA or double-stranded DNA with significant 3′ overhangs (Ma et al., 2004; Yoon et al., 2005). We therefore postulated that the SET complex might contain an exonuclease. Here we show that the 3′-to-5′ exonuclease TREX1/DNase III (Höss et al., 1999; Mazur and Perrino, 1999) is a component of the SET complex. Inclusion of TREX1 in the SET complex is specific, since the

*Correspondence: lieberman@cbr.med.harvard.edu
[4] Present address: Department of Biology, Dongguk University, Seoul 100-715, Korea.

TREX1 homolog TREX2 (44% identity) (Mazur and Perrino, 1999) is not in the complex. TREX1, like NM23-H1, is not a GzmA substrate. On its own, TREX1 does not damage intact DNA. It acts in concert with NM23-H1 to destroy DNA during GzmA-mediated cell death. After NM23-H1 nicks one strand, TREX1 removes bases from the free 3′ end to enhance the damage and prevents DNA end reannealing and rapid repair.

Results

The SET Complex Contains the Exonuclease TREX1

The SET complex was previously identified and purified from cytoplasmic lysates by sequential binding to immobilized enzymatically inactive S-AGzmA (mutated at the active site Ser→Ala), followed by gel filtration on a Sephacryl 400 column (Beresford et al., 1997, 2001). To increase the yield of the purified complex, we took advantage of the homotypic binding of SET (Miyaji-Yamaguchi et al., 1999), to replace the GzmA affinity-purification step with binding to immobilized recombinant SET. The known components of the SET complex, including SET, pp32, and NM23-H1, coeluted in a single broad peak between ~250 and 440 kDa (Figures 1A–1C). Like the previously purified SET complex (Beresford et al., 2001), the S400 fractions also degraded plasmid DNA on prolonged incubation (Figure 1B). After 48 hr, the intact supercoiled plasmid band began to disappear and was replaced by a more rapidly migrating smear of shorter nicked DNA. During the 2 day incubation, the inhibitor SET may have transiently dissociated from some NM23-H1 molecules, allowing some nicking to occur. Although the endonuclease NM23-H1 is reported to have limited exonuclease activity on single-stranded DNA and double-stranded DNA with significant 3′ overhang substrates (Ma et al., 2004; Yoon et al., 2005), we investigated whether the purified SET complex might contain other exonucleases. The 3′-to-5′ exonuclease TREX1/DNase III coelutes in fractions 68–72 with NM23-H1, SET, and pp32 (Figure 1C). TREX1 was also present in the SET complex eluted from the S-AGzmA affinity column (data not shown). TREX2, a TREX1 homolog, is not part of the SET complex. Another exonuclease, Exo1, also was not present in the complex.

NM23-H1 Is Not the SET Complex Exonuclease

The intact SET complex has limited nuclease activity that is detected only by prolonged (~2 day) incubation with plasmid DNA (Fan et al., 2003a) (Figure 1B). We previously showed that the nuclease activity of the intact complex is blocked by the SET protein, which inhibits the NM23-H1 endonuclease. The SET complex nuclease can be separated from the acidic SET and pp32 proteins by passage through an anion exchange Q column. We verified this result, as shown by Figure 1D. SET and pp32 bind to the column, while NM23-H1, Ape1, and HMG-2 are in the Q flowthrough (QFT) (Fan et al., 2003a) (Figure 1D). Although TREX1 binds to some extent to the Q column and is eluted with SET in the Q column eluate (QE), most TREX1 is in the QFT (Figure 1D). Because TREX1 is an exonuclease and NM23-H1 has also been reported to have exonuclease activity (Ma et al., 2004; Yoon et al., 2005), we wanted to determine which protein is responsible for the exonuclease activity of the QFT fractions of the SET complex. We therefore used immunodepletion with immobilized anti-NM23-H1 to separate NM23-H1 and TREX1 in the QFT (Figure 1D). TREX1 remained in the supernatant and did not coprecipitate with NM23-H1, suggesting that the two proteins do not interact directly. Control IgG beads did not deplete either TREX1 or NM23-H1. The control IgG supernatant that contains both TREX1 and NM23-H1 had unaltered QFT exonuclease activity. However, neither the NM23-H1 immunoprecipitate, lacking TREX1, nor the NM23-H1 supernatant, containing TREX1 but lacking NM23-H1, demonstrated exonuclease activity on plasmid DNA (Figure 1D). The NM23-H1 immunoprecipitate, however, did produce a band corresponding to nicked plasmid DNA. These results show that NM23-H1 is not the SET complex exonuclease. They suggest that TREX1 is the SET complex exonuclease but that TREX1 by itself is inactive against a circular plasmid and requires NM23-H1 to generate a nicked substrate for its activity.

Because TREX1 copurifies with the SET complex, we wanted to verify the association of SET and TREX1 within cells by coimmunoprecipitation experiments. K562 cell lysates immunoprecipitated with SET peptide antisera also reacted with antisera to TREX1, but not TREX2 (Figure 1E, top). To determine whether TREX1 interacts directly with SET, we attempted to coimmunoprecipitate the recombinant proteins. Recombinant SET coprecipitated with recombinant TREX1, but not TREX2 (Figure 1E, left), suggesting that TREX1 interacts directly with SET. However, the SET-TREX1 binding may be weak, since only a fraction of the TREX1 input material was brought down by the SET antisera. This suggests that other components of the SET complex may also interact with TREX1 and stabilize the interaction. TREX1 did not bind directly to recombinant pp32 or recombinant NM23-H1, demonstrating the specificity of the SET-TREX1 interaction (Figure 1E, right; data not shown). These results suggest that TREX1 is a component of the SET complex, potentially responsible for its exonuclease activity.

TREX1 Is Not a GzmA Substrate

Since TREX1 is contained in a GzmA-interacting complex, it might be a GzmA substrate like the SET complex proteins SET (Beresford et al., 2001), Ape1 (Fan et al., 2003b), and HMG-2 (Fan et al., 2002). Alternatively, it might be resistant to GzmA and play a role in GzmA-mediated cell death like the endonuclease NM23-H1 (Fan et al., 2003a). K562 cells were loaded with increasing concentrations of GzmA and incubated for different times. TREX1 was not degraded using GzmA concentrations as high as 1 μM or incubation for as long as 2 hr, whereas SET cleavage was seen with 10-fold less GzmA and within 15 min (Figure 2A). Furthermore, a molar excess of GzmA does not cut recombinant TREX1 in vitro (Figure 2B). Under the same conditions, GzmA cuts SET at low concentrations.

SET Does Not Inhibit the TREX1 Exonuclease

In our previous study, we found that SET inhibits the endonuclease activity of NM23-H1 (Fan et al., 2003a). Since SET interacts directly with TREX1, we wanted to determine whether SET affects TREX1 exonuclease

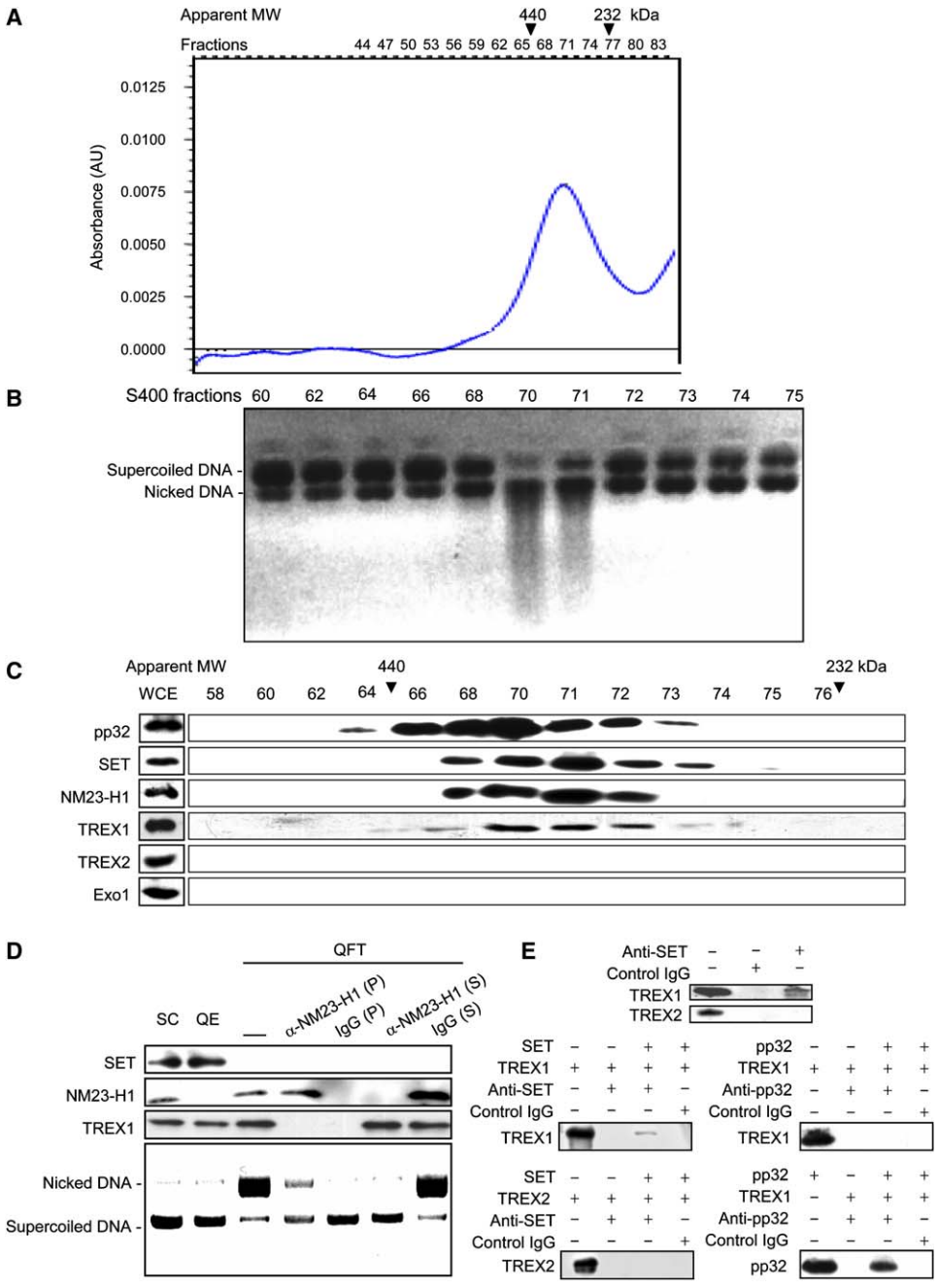

Figure 1. TREX1 Coelutes and Coimmunoprecipitates with the SET Complex

(A) A 250–420 kDa complex elutes from K562 cytoplasmic lysates applied sequentially to immobilized SET and S400 gel filtration columns. Migration of the 232 kDa and 440 kDa gel filtration standards is shown.

(B) Nuclease activity coincides with S400 fractions containing the 250–420 kDa complex. Fractions obtained as in (A) were incubated with plasmid DNA at 37°C for 48 hr and electrophoresed through agarose gels.

(C) TREX1 copurifies with the SET complex proteins SET, pp32, and NM23-H1. S400 fractions were analyzed by immunoblot with antibodies against the SET complex proteins SET, pp32, and NM23-H1 and the exonucleases TREX1, TREX2, and Exo1. WCE, whole-cell extract.

(D) TREX1 and NM23-H1 are both required for the exonuclease activity of the SET complex (SC). The SET complex, isolated by gel filtration as above, was further fractionated by ion-exchange chromatography using Q beads. The top three panels depict immunoblots probed for SET, NM23-H1, and TREX1. The Q eluate (QE) contains SET and low levels of TREX1. The Q flowthrough (QFT) has NM23-H1 and higher amounts of TREX1. NM23-H1 was immunoprecipitated (α-NM23-H1[P]) from the QFT using anti-NM23-H1 antibody. The supernatant (α-NM23-H1[S]) contains TREX1. The control IgG does not immunoprecipitate NM23-H1 or TREX1 (IgG [P]), and both proteins are in the supernatant (IgG [S]). These fractions were incubated with plasmid DNA for 2 hr at room temperature and electrophoresed through agarose gels (bottom panel).

(E) TREX1 binds directly to SET, but not to pp32, and associates with SET in K562 cell lysates. K562 cell lysates were immunoprecipitated with anti-SET antibody or control IgG and probed for TREX1 or TREX2 (top). Recombinant TREX1 or TREX2 was incubated with SET (left), or recombinant TREX1 was incubated with pp32 (right) and then immunoprecipitated with anti-SET or anti-pp32 antibody, respectively, or with control IgG. Immunoblots were probed for TREX1, TREX2, or pp32. TREX1 only binds to SET directly and not to pp32. TREX2 does not bind to SET directly or associate with SET in K562 cell lysates.

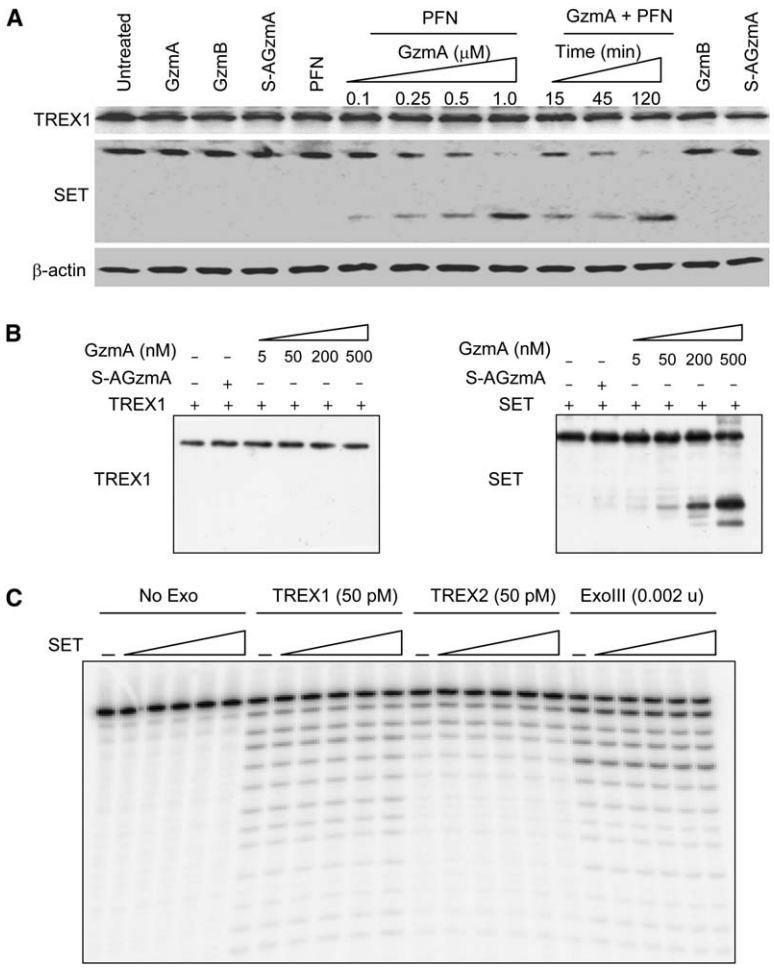

Figure 2. TREX1 Is Not a GzmA Substrate

(A) TREX1 is not cleaved by GzmA when K562 cells are loaded with GzmA and PFN for indicated times. Gzm concentration was 1 μM, except where indicated. SET is cleaved under these conditions.

(B) Recombinant TREX1 is not cleaved by GzmA. Recombinant TREX1 (left) or SET (right) (1 μM) was incubated for 2 hr at 37ºC with the indicated amounts of GzmA or 500 nM of S-AGzmA, and the reaction products were analyzed by TREX1 and SET immunoblot.

(C) SET does not affect the 3′-to-5′ exonuclease activity of TREX1. ^{32}P-labeled nicked double-stranded DNA substrate (10 nM) was incubated with 50 pM of recombinant TREX1 or TREX2 or 0.002 units of ExoIII in the presence of increasing amounts of SET (0, 0.01, 0.1, 1, 10, and 100 nM) at 30ºC for 10 min.

activity. We confirmed previous findings (Höss et al., 1999; Mazur and Perrino, 1999) that TREX1 is a potent 3′-to-5′ exonuclease and works efficiently on different double-stranded DNA substrates (data not shown). To mimic the physiological setting of NM23-H1 nicked DNA, a nicked DNA double-stranded substrate was used for the exonuclease assays. SET had no effect on the exonuclease activity of TREX1 (Figure 2C). The exonuclease activities of TREX2 and the bacterial exonuclease III (ExoIII), used as controls, were also unaffected by adding SET. Exonuclease activity of purified TREX1 is inhibited by NaCl concentrations above 50 mM (Mazur and Perrino, 2001a). The presence of SET also did not alter TREX1 activity in the presence of added salt (data not shown).

TREX1 Works in Concert with NM23-H1 to Degrade Plasmid DNA

We have previously shown by in vitro assays that NM23-H1 nicks plasmid DNA and that SET inhibits the nicking activity of NM23-H1 (Fan et al., 2003a). TREX1 does not have endonuclease activity and needs a free 3′-OH end to degrade DNA. We hypothesized that, during GzmA-mediated cell death, TREX1 accentuates the breaks made by NM23-H1 but cannot cause a break by itself. To test this hypothesis, we incubated supercoiled plasmid DNA with TREX1 and/or NM23-H1 (Figure 3A) at room temperature for 2 hr. Increasing amounts of NM23-H1 caused an increase in the nicked form of plasmid DNA but did not lead to its degradation. TREX1 alone did not cause changes in any form of DNA. TREX1 and NM23-H1 together worked in synergy and caused a significant decrease in total plasmid DNA levels. Addition of equimolar amounts of recombinant SET into this mix prevented the degradation of plasmid DNA, presumably by inhibiting the formation by NM23-H1 of nicked DNA, which is the substrate for TREX1. Furthermore, GzmA released the SET-mediated inhibition by cleaving SET (data not shown) and allowing NM23-H1 and, consequently, TREX1 to degrade plasmid DNA (Figure 3A, last lane). Although TREX1 and NM23-H1 degraded plasmid DNA, the smear expected for degradation by an exonuclease, seen in previous experiments (i.e., Figure 1D), was not visualized. The plasmid DNA may have been completely digested because the reaction proceeded rapidly at room temperature. Therefore, the experiment was repeated at 4ºC to slow the reaction rate. At 4ºC, the nicked band formed by NM23-H1 alone became a smear in the presence of increasing amounts of TREX1 (Figure 3B, upper panel). Another 3′-to-5′ exonuclease, bacterial ExoIII, when added with NM23-H1 caused a similar degradation pattern as TREX1. This confirms that TREX1 is indeed providing 3′-to-5′ exonuclease activity, which is necessary for DNA degradation. (It is worth noting that supercoiled DNA migrated more slowly than nicked DNA in the presence of ethidium

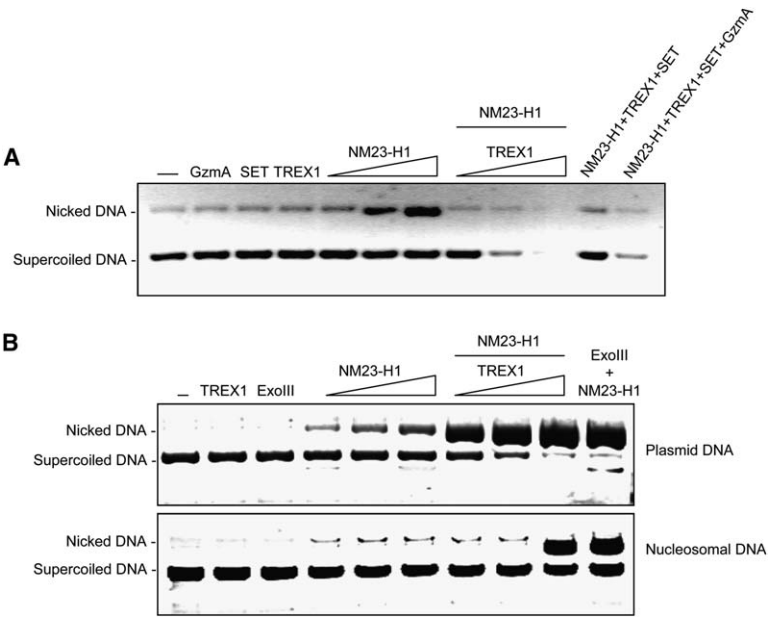

Figure 3. TREX1 Works in Concert with NM23-H1 to Degrade Both Plasmid and Nucleosomal DNA

(A) TREX1 and NM23-H1 act synergistically to degrade plasmid DNA. Plasmid pcDNA3 (0.5 μg) was incubated for 2 hr at room temperature with increasing amounts (12.5, 25, and 50 nM) of NM23-H1 or with 50 nM NM23-H1 in combination with increasing amounts (12.5, 25, and 50 nM) of TREX1. SET (50 nM) and/or GzmA (1 μM) were added to the reactions. The nicked form of the plasmid DNA increased with increasing amounts of NM23-H1. TREX1 is inactive in the absence of nicking by NM23-H1; moreover, the NM23-H1-nicked DNA is not degraded in the absence of TREX1. Only the combination of TREX1 and NM23-H1 degrades both nicked and supercoiled DNA.

(B) TREX1 is necessary to degrade nucleosomal DNA. Plasmid DNA (upper panel) and nucleosomal DNA (lower panel) were incubated for 2 hr at 4ºC with increasing amounts (as in [A]) of NM23-H1 and TREX1. The lower temperature decreases the reaction rate, allowing visualization of degraded DNA intermediates. Nucleosomal DNA was visibly degraded only at the highest concentration of TREX1 (50 nM) and NM23-H1 (50 nM). Bacterial ExoIII (5 units) was used as a control exonuclease.

bromide in Figure 1B but migrated faster in the absence of ethidium bromide in Figures 3 and 1D).

Because DNA is incorporated into nucleosomes within the cell, we next wanted to know whether NM23-H1 and TREX1 are active on chromatinized DNA (Figure 3B, lower panel). NM23-H1 and TREX1 also nicked and degraded nucleosomal DNA at 4ºC. As expected, nucleosomal DNA was more resistant to nuclease digestion than plasmid DNA, and a DNA smear was apparent only at the highest concentration of TREX1. Together, these results suggest that both TREX1 and NM23-H1 are necessary for efficient degradation of DNA and that they work synergistically.

TREX1 Colocalizes with NM23-H1 and Cotranslocates to the Nucleus in Response to GzmA

In untreated HeLa cells, NM23-H1 and the SET complex are primarily perinuclear and associate with the endoplasmic reticulum (Fan et al., 2003a). However, when cells are treated with GzmA and PFN, NM23-H1 rapidly translocates to the nucleus (Fan et al., 2003a; Martinvalet et al., 2005). From our earlier experiments, we hypothesized that TREX1 works in concert with NM23-H1 within cells, which suggests that the two proteins should colocalize during GzmA-mediated cell death. Untreated, GzmA-treated, or PFN-treated HeLa cells costained for NM23-H1 and TREX1 in a predominantly perinuclear pattern. In contrast, in cells treated with GzmA and PFN for 20 min, much of the signal for the two proteins colocalized to the nucleus (Figure 4A and see Figure S1 in the Supplemental Data available with this article online). Immunostaining of β-actin as a control showed that β-actin remained mostly cytoplasmic under the same conditions in which TREX1 and NM23-H1 had cotranslocated to the intranuclear compartment (Figure 4A).

Although purified TREX1 and NM23-H1 do not interact directly in vitro (Figure 1D), we wanted to verify that TREX1 associates with NM23-H1 within cells and to find out whether they continue to associate during GzmA-mediated cell death. Hence, we did coimmunoprecipitation experiments using fractionated cell lysates (Figure 4B). Prior to treatment with GzmA and PFN, TREX1 and NM23-H1 coprecipitated using the NM23-H1 antibody and were detected in the cytoplasm and not in the nucleus. However, after GzmA and PFN treatment, the two proteins still coprecipitated, but now much of the signal was detected in the nuclear fraction. TREX2 did not coprecipitate with NM23-H1 before or after GzmA/PFN treatment. The coimmunoprecipitation and colocalization of NM23-H1 and TREX1 and their nuclear translocation during GzmA-mediated cell death strongly suggest that the two proteins work together in this cell death pathway.

Silencing *TREX1* Inhibits GzmA-Mediated DNA Damage and Cell Death

To investigate the role of TREX1 in GzmA-mediated cell death, we silenced the expression of *TREX1* using two siRNA duplexes. We previously demonstrated that cells with diminished NM23-H1 protein are significantly more resistant to GzmA-mediated cell death (Fan et al., 2003a). We wanted to confirm this result and also to see whether silencing *TREX1*, alone or together with *NM23-H1*, increases the capacity of the cell to resist GzmA-mediated cell death. When siRNA duplexes targeting *NM23-H1* and/or *TREX1* were transfected into HeLa cells, the corresponding NM23-H1 and/or TREX1 proteins were decreased by >90% 3 days later (Figure 5A). Cells transfected with control siRNA against GFP had unchanged expression of both proteins. TREX2 and the ATR-interacting protein ATRIP, encoded

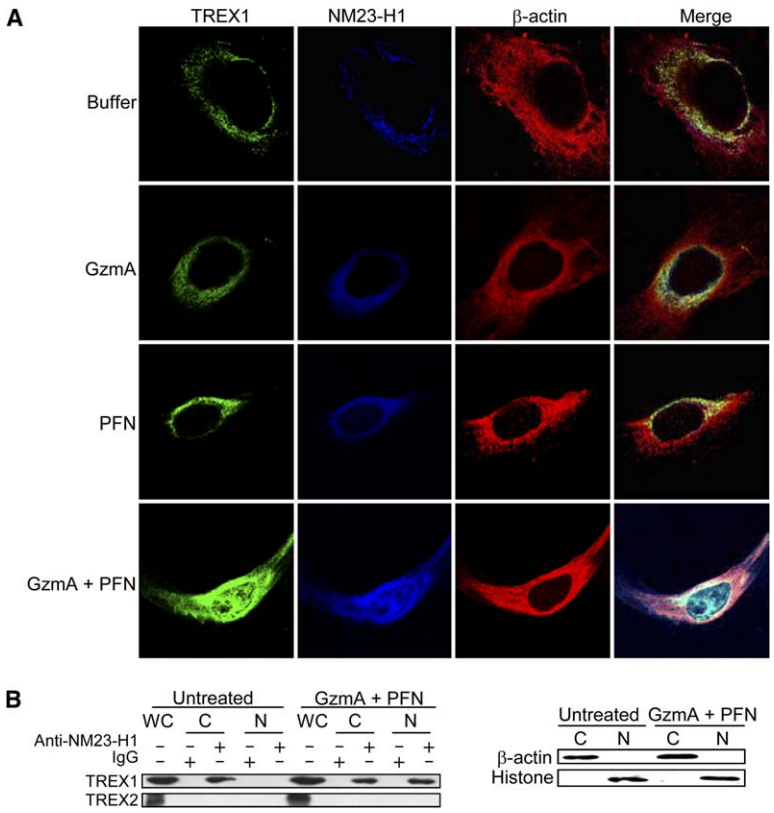

Figure 4. TREX1 Colocalizes with NM23-H1 and Interacts with It in the Nucleus of GzmA- and PFN-Treated Cells

(A) TREX1 colocalizes with NM23-H1 in the perinuclear region of cells, and they both partially translocate to the nucleus after GzmA and PFN treatment. HeLa cells treated for 25 min with GzmA and/or PFN were stained for NM23-H1 and TREX1. TREX1 and NM23-H1 partially translocate to the nucleus after GzmA and PFN treatment, but β-actin remains in the cytoplasm.

(B) TREX1 physically associates with NM23-H1 in the nucleus of GzmA- and PFN-treated cells. Cytoplasmic (C) and nuclear (N) fractions or whole-cell lysates (WC) from untreated K562 cells or cells treated with GzmA and PFN as above were immunoprecipitated with NM23-H1 antibody or rabbit IgG and probed for TREX1. Cytoplasmic and nuclear fractions were immunoblotted with histone and β-actin antibody to verify cell fractionation.

by an upstream ORF from the same gene locus as *TREX1* (http://www.ncbi.nih.gov/LocusLink/LocRpt.cgi?l=11277), were also unchanged by the TREX1 siRNAs (data not shown). Cells with silenced *TREX1* or *NM23-H1* had comparable background Klenow labeling in the absence of GzmA treatment (data not shown) or upon treatment with inactive S-AGzmA, which served as a negative control. However, cells with silenced *TREX1* or *NM23-H1* had significantly fewer DNA breaks (measured by Klenow labeling) after GzmA treatment of cell lysates, relative to cells treated with *GFP* siRNA ($p < 0.001$) (Figure 5B). However, DNA damage was not further reduced when both *TREX1* and *NM23-H1* were silenced. This suggests that NM23-H1 and TREX1 work together in the same pathway to cause DNA damage, rather than in parallel pathways.

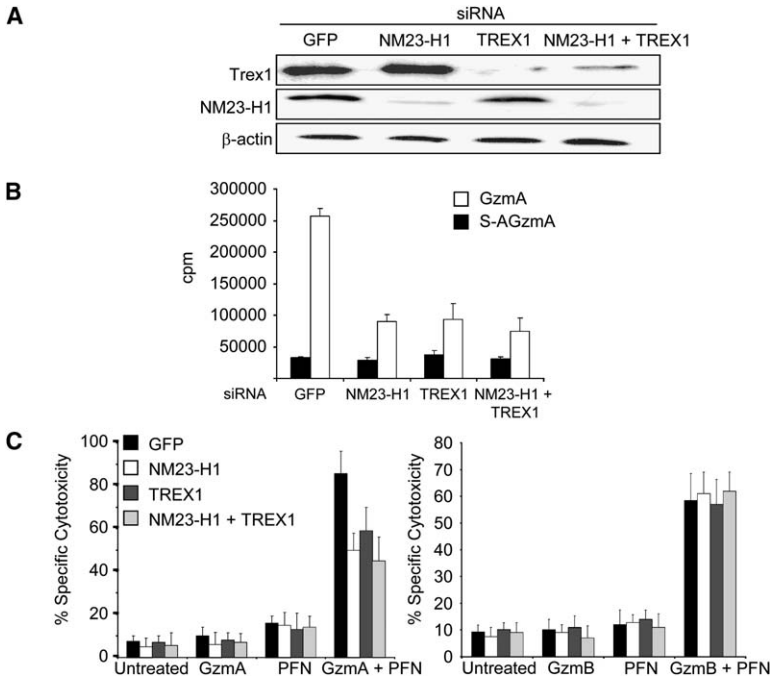

Figure 5. Silencing *TREX1* and/or *NM23-H1* Expression Decreases GzmA-Induced DNA Damage and Cell Death

(A) *TREX1* and *NM23-H1* expression are silenced in HeLa cells after treatment with siRNA duplexes against *TREX1* and *NM23-H1*. β-actin expression remains unchanged.

(B) *TREX1* and *NM23-H1* silencing significantly diminishes GzmA-mediated DNA damage in isolated HeLa nuclei, as measured by radionucleotide incorporation at nicked DNA using Klenow DNA polymerase. White bars indicate mean ±SD for GzmA-treated nuclei, and black bars indicate S-AGzmA-treated nuclei.

(C) HeLa cells with silenced *TREX1* and *NM23-H1* expression are more resistant than control cells to cell death induced by GzmA (left), but not by GzmB (right), as assayed by ^{51}Cr release. The effect of silencing expression of both proteins on GzmA-induced DNA damage or cytolysis is not significantly different from silencing either one of the proteins. Data shown are the means ±SD of at least three independent experiments with HeLa cells either transfected with control *GFP* siRNA or *NM23-H1* and *TREX1* siRNA individually or together.

To determine whether silencing *TREX1* interferes with GzmA-mediated cell death, as well as with DNA damage, ^{51}Cr-labeled HeLa cells with silenced *TREX1* and/or *NM23-H1* were loaded with GzmA and PFN (Figure 5C). Cells with silenced *TREX1* and/or *NM23-H1* demonstrated no change in background cytolysis with no additional treatment or following treatment with GzmA or PFN alone. However, *TREX1* and/or *NM23-H1* silenced cells were substantially less sensitive to cell death caused by treatment with GzmA and PFN than cells pretreated with the control *GFP* siRNA ($p < 0.002$). Cells with silenced TREX1 were comparable to cells with silenced *NM23-H1* in their resistance to GzmA-activated death. Consistent with the previous result (Figure 5B), cells that had both genes silenced were as sensitive to cytolysis as cells with either *NM23-H1* or *TREX1* silenced. Silencing *TREX2* had no effect on GzmA- or GzmB-mediated cell death (Figure S2).

Silencing *TREX1* or *NM23-H1* Does Not Affect GzmB-Induced Cell Death

Since GzmB can cause caspase-independent, as well as caspase-dependent, cell death, we wanted to investigate whether TREX1 and NM23-H1 play any role in the GzmB pathway. When cells transfected with *NM23-H1* siRNA and/or *TREX1* siRNA were treated with GzmB and PFN, silencing either *TREX1*, or *NM23-H1*, or both made no difference to GzmB-mediated cytolysis (Figure 5C). The specific importance of TREX1 and NM23-H1 in the GzmA pathway was verified by measuring cytolysis by granules purified from the human NK cell line, YT-INDY, which expresses GzmB but does not express GzmA (Su et al., 1994). Cytotoxic granules from YT-INDY cells lysed HeLa cells transfected with *GFP* siRNAs or with *TREX1* and/or *NM23-H1* siRNAs with comparable efficiency, thus demonstrating that TREX1 and NM23-H1 are specifically involved in GzmA-mediated cell death (Figure S3).

Discussion

GzmA induces cell death via a caspase-independent pathway, which uniquely among cell death pathways involves single-stranded DNA damage (Beresford et al., 1999; Shresta et al., 1999). We previously identified the endonuclease (NM23-H1) as a GzmA-activated DNase responsible for causing the single-stranded DNA breaks (Fan et al., 2003a) (Figure 6). NM23-H1 is found in the SET complex with its specific inhibitor, SET. GzmA cleaves SET, releasing its inhibition of NM23-H1. In that report, we had speculated that other nucleases might contribute to DNA damage initiated by GzmA. We now find that DNA damage by GzmA is enhanced by another component of the SET complex, the exonuclease TREX1, which acts to remove nucleotides from free 3′-OH ends formed by NM23-H1 nicks. Single-stranded DNA nicks can be repaired relatively quickly by the base excision repair (BER) machinery (Demple and DeMott, 2002; Krokan et al., 2000). One way that GzmA deals with this challenge is by cleaving and inactivating Ape1 (Fan et al., 2003b), a key enzyme in BER, also contained in the SET complex. In this study, we show another tactic of the GzmA pathway for interfering with the repair of DNA breaks, which also involves the SET complex. We demonstrate both in vitro and in vivo that TREX1 and NM23-H1 work together, with NM23-H1 causing the initial nick to create the appropriate substrate for TREX1. TREX1 then further degrades the nicked DNA, causing irreparable damage. Consistent with this role of TREX1 in enhancing NM23-H1-induced DNA damage, we find that TREX1 is closely associated with NM23-H1 in the SET complex and translocates with it from the cytoplasm to the nucleus when cells are treated with GzmA. We previously showed that superoxide generated by GzmA mitochondrial damage causes nuclear relocation of the SET complex (Martinvalet et al., 2005). Furthermore, GzmA does not cleave TREX1, so its exonuclease activity remains intact. Silencing *TREX1* renders cells relatively resistant to GzmA-activated DNA damage and cell death, providing further evidence for the importance of TREX1 in GzmA-activated DNA damage. Moreover, silencing *NM23-H1* at the same time as *TREX1* does not add to GzmA resistance, in support of the hypothesis that the exonuclease acts in the same pathway to extend the break caused by NM23-H1 nicking. The close association of TREX1 and NM23-H1, which can be coimmunoprecipitated from nuclear fractions after GzmA loading, further supports the idea that the two nucleases work in concert during GzmA-mediated cell death. Only a limited number of factors have been implicated in caspase-independent apoptotic pathways. TREX1 is a new addition to that short list.

The purified SET complex has exonuclease activity on plasmid DNA, which is accelerated by GzmA treatment, presumably via removing SET inhibition. Recently, mammalian NM23-H1 expressed in bacteria was also found to have weak 3′-to-5′ exonuclease activity (Ma et al., 2004; Yoon et al., 2005). Because of the close association of NM23-H1 with an exonuclease in mammalian cells, it is possible that the highly conserved NM23-H1, which is homologous to ndk in bacteria, might associate with the DnaQ protein of the DNA polymerase III holoenzyme, the bacterial homolog of TREX1. Trace amounts of a contaminating bacterial exonuclease might lead to the erroneous conclusion that NM23-H1 has exonuclease activity. In light of this study, the weak exonuclease activity of NM23-H1 should be reexamined. Optimal exonuclease activity of NM23-H1 on double-stranded DNA substrates is only achieved in concert with Ape1 and a DNA glycosylase (Yoon et al., 2005). Since GzmA cleaves and inactivates Ape1 (Fan et al., 2003b), that in turn will severely impede any exonuclease activity of NM23-H1. In this study, we found that the exonuclease activity of the SET complex did not fractionate with NM23-H1 (Figure 1D). Hence, NM23-H1 is unlikely to be responsible for the exonuclease activity of the GzmA-treated SET complex.

The functions of TREX1 and of the SET complex in normal cellular metabolism are unknown. TREX1 was isolated as the most abundant 3′-to-5′ exonuclease in cells (Höss et al., 1999; Mazur and Perrino, 1999). It is ubiquitously expressed, as is the SET complex. Early experiments proposed a role for TREX1 in providing proofreading activity for DNA Polβ, a key factor in BER. In a reconstituted mammalian DNA-repair system containing DNA Polβ, accurate rejoining of a 3′ mismatched base residue at a single-strand break depended on addition

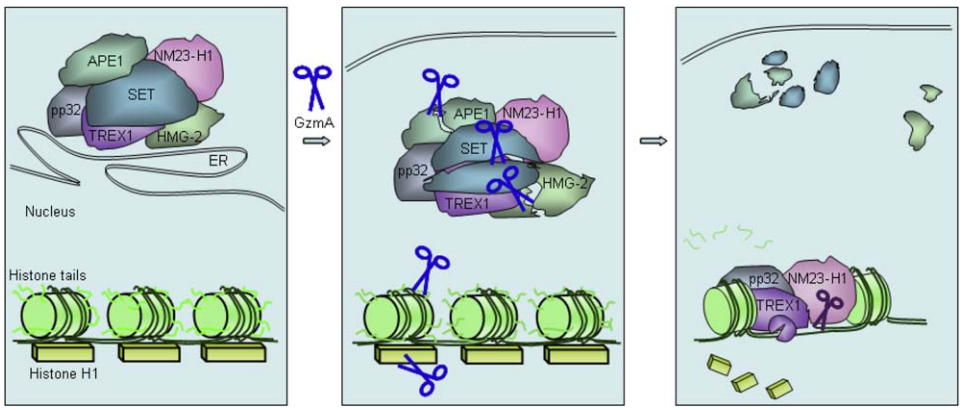

Figure 6. Model for GzmA-Induced DNA Damage

The SET complex, normally associated with the endoplasmic reticulum (ER) (left panel), translocates to the nucleus in response to mitochondrial damage and superoxide generation when cells are treated with GzmA (Martinvalet et al., 2005) (middle panel). GzmA cleaves SET, Ape1, and HMG-2 in the SET complex as well as histone H1 and the tails of the core histones (Beresford et al., 1997; Fan et al., 2002; Fan et al., 2003b; Zhang et al., 2001b). Cleaving the histones opens up chromatin and makes it more accessible to DNases (Zhang et al., 2001b) (right). SET is an inhibitor of NM23-H1. After GzmA cleaves SET, NM23-H1 is able to nick one strand of the DNA (Fan et al., 2003a). The 3′-to-5′ exonuclease TREX1, another component of the SET complex, then extends the cut.

of TREX1 (Höss et al., 1999). DNA Polβ is a highly error-prone polymerase that does not have intrinsic exonuclease activity (Osheroff et al., 1999). Since a high error frequency would not be acceptable during DNA repair, a separate 3′ exonuclease may be needed to work in concert with DNA Polβ. The sequence homology between TREX1 and the DnaQ protein of the DNA polymerase III holoenzyme in *E. coli* and of the 3′ exonuclease domain of eukaryotic Polε made this an attractive proposition (Höss et al., 1999; Scheuermann and Echols, 1984). However, genetic deletion of *TREX1* does not cause an increased frequency of spontaneous mutation or cancer (Morita et al., 2004), suggesting that TREX1 might not have a role in BER. It is noteworthy that TREX2, a close homolog of TREX1, has the same substrate specificity as TREX1 (Mazur and Perrino, 2001a) and can potentially substitute for TREX1 in TREX1-deficient cells. Hence, it remains to be seen whether a deficiency in both these exonucleases impedes BER. Our finding TREX1 in a complex with Ape1 lends support to the hypothesized role of TREX1 as a proofreading exonuclease for BER. Moreover, NM23-H1 may have DNA glycosylase and lyase activities normally associated with BER, although this is controversial (Bennett et al., 2004; Postel and Abramczyk, 2003). Since Ape1 and possibly TREX1 and NM23-H1 in the SET complex may have functions in BER, and since the SET complex is mobilized to the nucleus in response to oxidative damage, which causes DNA lesions that are repaired by BER, our findings suggest that the SET complex might be a BER complex.

The SET complex may play a role in BER or other DNA-repair pathways only under certain cellular conditions. Although Ape1 is a component of the SET complex, it also is widely distributed in the nucleus of unstressed cells under conditions in which the SET complex is extranuclear. Therefore, one possibility is that, under normal circumstances, BER occurs independently of the SET complex, utilizing either the weak exonuclease activity of Ape1 (Chou and Cheng, 2002), although this is unlikely (Wong et al., 2003), or another exonuclease, such as TREX2, for proofreading. The SET complex may serve as a reservoir for Ape1 and other BER factors that are mobilized into the nucleus only under extreme conditions of oxidative stress. The SET complex proteins SET and pp32 have well-documented roles in regulating DNA replication and histone acetylation (Nagata et al., 1995; Seo et al., 2001), whereas HMG-2 is a DNA-binding protein with specificity for distorted secondary structures (Bustin, 1999). These factors could potentially contribute to influencing chromatin structure during BER or other DNA-repair events. We envisage a scenario in which SET, pp32, and HMG-2 alter chromatin structure at the site of DNA damage. These alterations in chromatin structure may actually help target the DNA-repair factors Ape1, NM23-H1, and TREX1 to DNA-damage sites. If that is the case, then a potential role for TREX1 in BER in *TREX1*$^{-/-}$ mice might only become evident if animals are subjected to extraordinary oxidative stress. According to this hypothesis, exogenous GzmA would then hijack this DNA-repair complex and convert it into an engine for irreversible DNA damage.

Experimental Procedures

Cell Lines and Antibodies

K562 cells and YT-INDY cells were grown in RPMI 1640, and HeLa cells were grown in DMEM supplemented with 10% fetal calf serum, 2 mM glutamine, 2 mM HEPES, 100 units/ml of penicillin, and 100 mg/ml of streptomycin. Mouse pp32 mAb (RJ1) and SET rabbit antiserum were described (Beresford et al., 2001). TREX1 and TREX2 antibodies were generated commercially in multiple rabbits (Rockland Immunochemicals, Gilbertsville, Pennsylvania), using purified TREX1 and TREX2 proteins. Antibodies for NM23-H1 (rabbit polyclonal, Santa Cruz), TREX1 (monoclonal, BD Transduction Labs), Exo1 (monoclonal, AbCam), actin (goat polyclonal, Santa Cruz), β-actin (monoclonal, Sigma), and panhistone (monoclonal, Chemicon International) were purchased. Antibody for ATRIP (rabbit polyclonal) was kindly provided by S. Elledge (Harvard Medical School).

Recombinant Proteins and Purified PFN

Recombinant GzmA, inactive S-AGzmA, and GzmB were produced and purified as previously described (Beresford et al., 1999). PFN was purified from the rat RNK-16 cell line and used at a sublytic concentration as described previously (Shi et al., 1992). Recombinant

SET, pp32, and NM23-H1 were expressed in BL21-DE3 cells and purified as described (Fan et al., 2003a). TREX1 and TREX2 proteins were purified as described (Mazur and Perrino, 2001b). *E. coli* ExoIII was purchased from New England Biolabs, and its unit activity was defined by the manufacturer.

Native SET Complex Purification

K562 cell lysates (10^{10} cells in Nonidet P-40 [NP-40] lysis buffer) were loaded onto an S-AGzmA column or SET affinity column as described (Beresford et al., 1999) and eluted with 500 mM NaCl in 50 mM Tris-HCl (pH 7.5). The concentrated eluate was applied in Tris-buffered saline (TBS) to a Sephacryl 400 gel filtration column (2.5 cm × 1.0 min; Pharmacia). Eluted fractions were analyzed by SDS-PAGE and immunoblotting and compared to the elution profile of Pharmacia gel filtration standards. The pooled S400 fractions were concentrated and incubated with equilibrated Q beads (Pharmacia) and eluted with 500 mM NaCl.

Coimmunoprecipitation

Coimmunoprecipitations of recombinant proteins were performed as described (Fan et al., 2002). Antibodies were preincubated with protein A agarose for 1 hr at 4ºC. The antibody-coated beads were washed and added to recombinant proteins (50 μg/ml) that had been preincubated for 2 hr at 4ºC. After overnight shaking, the beads were washed with 1% NP-40 and 0.1% SDS in TBS. Finally, the beads were boiled with SDS loading buffer and analyzed by SDS-PAGE and immunoblot. For coimmunoprecipitation from cell lysates, K562 cells (10^7) were untreated or treated with a sublytic dose of PFN and GzmA (1 μM) for 20 min. The cells were resuspended in low-salt buffer (10 mM NaCl, 10 mM Tris-Cl [pH 8], 1 mM DTT, and protease inhibitor cocktail) and dounced until they lysed. After centrifugation at 2000 rpm for 15 min, the supernatant (cytoplasmic fraction) was separated from the pellet (nuclear fraction). The pellet was resuspended in an equal volume of high-salt buffer (1.2 M NaCl, 40 mM Tris-HCl [pH 7.5], 2 mM DTT, and 20% glycerol). The crude nuclear extract was sonicated and centrifuged, and the supernatant was collected as the nuclear extract, which was diluted with 50 mM Tris-HCl (pH 8) to a final salt concentration of 200 mM. The diluted nuclear and cytoplasmic extracts were used for immunoprecipitation as above.

Plasmid and Nucleosomal DNA Digestion

Plasmid pcDNA3 (0.5 μg) was incubated in 20 μl of 50 mM Tris-HCl (pH 7.5), 1 mM EGTA, 5 mM $MgCl_2$, and 1 mg/ml bovine serum albumin at 37ºC for 48 hr with 10 μl of the indicated chromatography fractions, before deproteinization and analysis by agarose gel electrophoresis. In Figure 1B, ethidium bromide was added to samples before electrophoresis. Plasmid DNA digestion with the SET complex after Q bead fractionation and with indicated amounts of recombinant proteins (NM23-H1, TREX1, SET, and GzmA) was done under similar buffer conditions but for 2 hr at room temperature or at 4ºC as indicated. Nucleosomal arrays were reconstituted by salt dialysis of histone octamer with plasmid DNA as previously described (Logie and Peterson, 1999), and the nucleosome saturation was determined to be 60%–80% by digestion analysis. The nucleosomal DNA was incubated with indicated combinations of NM23-H1, TREX1, and ExoIII under above-mentioned buffer conditions at 4ºC for 2 hr.

GzmA Cleavage Assay

For in vitro cleavage, recombinant proteins (0.5 μM) were incubated for the indicated times at 37ºC with indicated concentrations of GzmA in 20 μl of 50 mM Tris-HCl (pH 7.5), 1 mM $CaCl_2$, and 1 mM $MgCl_2$. For cleavage in cells, cells were treated with a sublytic dose of PFN and indicated amounts of GzmA in loading buffer (HBSS with 1 mg/ml BSA, 1 mM $CaCl_2$, and 1 mM $MgCl_2$). Unless otherwise indicated, the GzmA concentration used to treat cells was chosen as the dose at which the cytotoxicity curve begins to plateau (1 μM for K562, 2.5 μM for HeLa). Cells were incubated for the indicated time at 37ºC. Both the in vitro and in vivo cleavage reactions were stopped by adding SDS loading buffer and boiling for 5 min. Samples were analyzed by SDS-PAGE and immunoblot.

Exonuclease Assay

DNA substrates for the exonuclease assay were prepared as described previously (Wong et al., 2003). Exonuclease reactions were performed in BER buffer (50 mM HEPES-KOH [pH 7.5], 8 mM $MgCl_2$, 5% [v/v] glycerol, 0.5 mM DTT, and 0.1 mg/ml BSA) with 10 nM DNA substrate incubated with indicated amounts of exonucleases and recombinant SET. After incubation at 30ºC for 10 min, the reactions were terminated by the addition of formamide loading buffer (90% formamide, 10 mM EDTA, bromophenol blue, and xylene cyanol) and boiling for 2 min. The DNA was resolved by acrylamide gels (14%) containing 7 M urea and analyzed using a phosphorimager (Molecular Image System, Bio-Rad).

Immunofluorescence

HeLa cells (2×10^5) grown overnight on coverslips were washed with HBSS and then left untreated or treated with GzmA (2.5 μM), PFN (sublytic dose), or both for 20 min in loading buffer. After an additional wash with HBSS, the cells were fixed with 3.7% paraformaldehyde for 30 min, neutralized with 50 mM NH_4Cl, permeabilized, and blocked at room temperature in 1× permeabilization/wash (P/W) buffer (BD Biosciences) containing 5% donkey serum. Antibodies were diluted in blocking buffer and incubated with samples at room temperature for 2 hr (primary antibodies) or 1 hr (secondary antibodies). After incubation with secondary antibodies, the cells were incubated with 0.5 μg/ml of propidium iodide and 100 μg/ml of Rnase A for 10 min. Samples were mounted with ProLong Antifade mounting medium, and images were acquired with a Bio-Rad Radiance 2000 laser scanning confocal microscope.

Silencing *TREX1* by RNA Interference

Silencing using synthetic 21 nt siRNA duplexes was performed as described (Fan et al., 2003a). *GFP* and *NM23-H1* siRNA sequences were previously described (Fan et al., 2003a). Two siRNA duplexes (Dharmacon) designed to silence *TREX1* were as follows: siRNA #1, sense 5′-CCAAGACCATCTGCTGTCA-3′, antisense 5′-TGACAGCAGATG GTCTTGG-3′; and siRNA #2, sense 5′-ACAATGGTGACCGCTAC GA-3′, antisense 5′-TCGTAGCGGTCACCATTGT-3′. Two siRNA duplexes (Dharmacon) designed to silence *TREX2*, but not *TREX1*, were as follows: siRNA #1, sense 5′-CATGTACTTGCCGCCTGAT-3′, antisense 5′-ATCAGGCGGCAAGTACATG-3′; and siRNA #2, sense 5′-CCCGGAGCACGACGAGTCT-3′, antisense 5′-AGACTCGT CGTGCTCCGGG-3′. HeLa cells were analyzed 3 days after transfection by immunoblot for TREX1, TREX2, and NM23-H1. For cytotoxicity assays, silenced or control-transfected cells were radiolabeled with ^{51}Cr for 1 hr and washed before loading with granzyme and PFN as above or with cytotoxic granules from YT-INDY cells. YT-INDY granules were purified using the previously described granule purification method (Davis et al., 2003). After 4 hr, ^{51}Cr release in the supernatant was measured on a Packard TopCount. Specific cytotoxicity was calculated using the equation 100 × ([sample release] – [spontaneous release]) / ([total release] – [spontaneous release]).

DNA-Nicking Assay

The Klenow fragment of DNA polymerase was used to label nicked DNA as described (Beresford et al., 1999). Cells (2×10^5) transfected with specific or control siRNAs were resuspended in 40 μl of HBSS with 1 mg/ml BSA, 2 mM $CaCl_2$, and 2 mM $MgCl_2$ before lysis in an equal volume of NP-40 lysis buffer. GzmA (1 μM) or S-AGzmA (3 μg in 20 μl of 140 mM NaCl, 10 mM HEPES [pH 7.2], and 1 mM EGTA) was added, and the treated lysates were incubated at 37ºC for 4 hr. Washed nuclear pellets were then incubated with 5 units of Klenow (New England Biolabs) and 10 μCi of [^{32}P] dATP in 10 μl of NP-40 lysis buffer at 37ºC for 1 hr. Radiolabeled nuclei, pelleted by centrifugation for 5 min at 2580 × g, were washed twice with NP-40 lysis buffer and counted after adding scintillation fluid.

Supplemental Data

Supplemental Data include three figures and can be found with this article online at www.molecule.org/cgi/content/full/23/1/133/DC1/.

Acknowledgments

This work was supported by NIH grants AI45587 (J.L.), GM069962 (F.W.P.), and GM40000 and CA71993 (B.D.) and by a Leukemia & Lymphoma Society fellowship to D.C. We thank L. Shi for providing perforin and M. Sinha (University of Massachusetts, Worcester) for providing histone octamer.

Received: December 23, 2005
Revised: April 27, 2006
Accepted: June 12, 2006
Published: July 6, 2006

References

Bennett, S.E., Chen, C.Y., and Mosbaugh, D.W. (2004). *Escherichia coli* nucleoside diphosphate kinase does not act as a uracil-processing DNA repair nuclease. Proc. Natl. Acad. Sci. USA *101*, 6391–6396.

Beresford, P.J., Kam, C.M., Powers, J.C., and Lieberman, J. (1997). Recombinant human granzyme A binds to two putative HLA-associated proteins and cleaves one of them. Proc. Natl. Acad. Sci. USA *94*, 9285–9290.

Beresford, P.J., Xia, Z., Greenberg, A.H., and Lieberman, J. (1999). Granzyme A loading induces rapid cytolysis and a novel form of DNA damage independently of caspase activation. Immunity *10*, 585–594.

Beresford, P.J., Zhang, D., Oh, D.Y., Fan, Z., Greer, E.L., Russo, M.L., Jaju, M., and Lieberman, J. (2001). Granzyme A activates an endoplasmic reticulum-associated caspase-independent nuclease to induce single-stranded DNA nicks. J. Biol. Chem. *276*, 43285–43293.

Bustin, M. (1999). Regulation of DNA-dependent activities by the functional motifs of the high-mobility-group chromosomal proteins. Mol. Cell. Biol. *19*, 5237–5246.

Chou, K.M., and Cheng, Y.C. (2002). An exonucleolytic activity of human apurinic/apyrimidinic endonuclease on 3′ mispaired DNA. Nature *415*, 655–659.

Davis, J.E., Sutton, V.R., Browne, K.A., and Trapani, J.A. (2003). Purification of natural killer cell cytotoxic granules for assaying target cell apoptosis. J. Immunol. Methods *276*, 59–68.

Demple, B., and DeMott, M.S. (2002). Dynamics and diversions in base excision DNA repair of oxidized abasic lesions. Oncogene *21*, 8926–8934.

Fan, Z., Beresford, P.J., Zhang, D., and Lieberman, J. (2002). HMG2 interacts with the nucleosome assembly protein SET and is a target of the cytotoxic T-lymphocyte protease granzyme A. Mol. Cell. Biol. *22*, 2810–2820.

Fan, Z., Beresford, P.J., Oh, D.Y., Zhang, D., and Lieberman, J. (2003a). Tumor suppressor NM23-H1 is a granzyme A-activated DNase during CTL-mediated apoptosis, and the nucleosome assembly protein SET is its inhibitor. Cell *112*, 659–672.

Fan, Z., Beresford, P.J., Zhang, D., Xu, Z., Novina, C.D., Yoshida, A., Pommier, Y., and Lieberman, J. (2003b). Cleaving the oxidative repair protein Ape1 enhances cell death mediated by granzyme A. Nat. Immunol. *4*, 145–153.

Griffiths, G.M. (2003). Endocytosing the death sentence. J. Cell Biol. *160*, 155–156.

Höss, M., Robins, P., Naven, T.J., Pappin, D.J., Sgouros, J., and Lindahl, T. (1999). A human DNA editing enzyme homologous to the *Escherichia coli* DnaQ/MutD protein. EMBO J. *18*, 3868–3875.

Krokan, H.E., Nilsen, H., Skorpen, F., Otterlei, M., and Slupphaug, G. (2000). Base excision repair of DNA in mammalian cells. FEBS Lett. *476*, 73–77.

Lieberman, J. (2003). The ABCs of granule-mediated cytotoxicity: new weapons in the arsenal. Nat. Rev. Immunol. *3*, 361–370.

Lieberman, J., and Fan, Z. (2003). Nuclear war: the granzyme A-bomb. Curr. Opin. Immunol. *15*, 553–559.

Logie, C., and Peterson, C.L. (1999). Purification and biochemical properties of yeast SWI/SNF complex. Methods Enzymol. *304*, 726–741.

Ma, D., McCorkle, J.R., and Kaetzel, D.M. (2004). The metastasis suppressor NM23-H1 possesses 3′-5′ exonuclease activity. J. Biol. Chem. *279*, 18073–18084.

Martinvalet, D., Zhu, P., and Lieberman, J. (2005). Granzyme A induces caspase-independent mitochondrial damage, a required first step for apoptosis. Immunity *22*, 355–370.

Mazur, D.J., and Perrino, F.W. (1999). Identification and expression of the TREX1 and TREX2 cDNA sequences encoding mammalian 3′→5′ exonucleases. J. Biol. Chem. *274*, 19655–19660.

Mazur, D.J., and Perrino, F.W. (2001a). Excision of 3′ termini by the Trex1 and TREX2 3′→5′ exonucleases. Characterization of the recombinant proteins. J. Biol. Chem. *276*, 17022–17029.

Mazur, D.J., and Perrino, F.W. (2001b). Structure and expression of the TREX1 and TREX2 3′ → 5′ exonuclease genes. J. Biol. Chem. *276*, 14718–14727.

Miyaji-Yamaguchi, M., Okuwaki, M., and Nagata, K. (1999). Coiled-coil structure-mediated dimerization of template activating factor-I is critical for its chromatin remodeling activity. J. Mol. Biol. *290*, 547–557.

Morita, M., Stamp, G., Robins, P., Dulic, A., Rosewell, I., Hrivnak, G., Daly, G., Lindahl, T., and Barnes, D.E. (2004). Gene-targeted mice lacking the Trex1 (DNase III) 3′→5′ DNA exonuclease develop inflammatory myocarditis. Mol. Cell. Biol. *24*, 6719–6727.

Nagata, K., Kawase, H., Handa, H., Yano, K., Yamasaki, M., Ishimi, Y., Okuda, A., Kikuchi, A., and Matsumoto, K. (1995). Replication factor encoded by a putative oncogene, set, associated with myeloid leukemogenesis. Proc. Natl. Acad. Sci. USA *92*, 4279–4283.

Osheroff, W.P., Jung, H.K., Beard, W.A., Wilson, S.H., and Kunkel, T.A. (1999). The fidelity of DNA polymerase beta during distributive and processive DNA synthesis. J. Biol. Chem. *274*, 3642–3650.

Postel, E.H., and Abramczyk, B.M. (2003). *Escherichia coli* nucleoside diphosphate kinase is a uracil-processing DNA repair nuclease. Proc. Natl. Acad. Sci. USA *100*, 13247–13252.

Scheuermann, R.H., and Echols, H. (1984). A separate editing exonuclease for DNA replication: the epsilon subunit of *Escherichia coli* DNA polymerase III holoenzyme. Proc. Natl. Acad. Sci. USA *81*, 7747–7751.

Seo, S.B., McNamara, P., Heo, S., Turner, A., Lane, W.S., and Chakravarti, D. (2001). Regulation of histone acetylation and transcription by INHAT, a human cellular complex containing the set oncoprotein. Cell *104*, 119–130.

Shi, L., Kraut, R.P., Aebersold, R., and Greenberg, A.H. (1992). A natural killer cell granule protein that induces DNA fragmentation and apoptosis. J. Exp. Med. *175*, 553–566.

Shresta, S., Graubert, T.A., Thomas, D.A., Raptis, S.Z., and Ley, T.J. (1999). Granzyme A initiates an alternative pathway for granule-mediated apoptosis. Immunity *10*, 595–605.

Su, B., Bochan, M.R., Hanna, W.L., Froelich, C.J., and Brahmi, Z. (1994). Human granzyme B is essential for DNA fragmentation of susceptible target cells. Eur. J. Immunol. *24*, 2073–2080.

Wong, D., DeMott, M.S., and Demple, B. (2003). Modulation of the 3′→5′-exonuclease activity of human apurinic endonuclease (Ape1) by its 5′-incised abasic DNA product. J. Biol. Chem. *278*, 36242–36249.

Yoon, J.H., Singh, P., Lee, D.H., Qiu, J., Cai, S., O'Connor, T.R., Chen, Y., Shen, B., and Pfeifer, G.P. (2005). Characterization of the 3′ → 5′ exonuclease activity found in human nucleoside diphosphate kinase 1 (NDK1) and several of its homologues. Biochemistry *44*, 15774–15786.

Zhang, D., Beresford, P.J., Greenberg, A.H., and Lieberman, J. (2001a). Granzymes A and B directly cleave lamins and disrupt the nuclear lamina during granule-mediated cytolysis. Proc. Natl. Acad. Sci. USA *98*, 5746–5751.

Zhang, D., Pasternack, M.S., Beresford, P.J., Wagner, L., Greenberg, A.H., and Lieberman, J. (2001b). Induction of rapid histone degradation by the cytotoxic T lymphocyte protease Granzyme A. J. Biol. Chem. *276*, 3683–3690.

Zhu, P., Zhang, D., Chowdhury, D., Martinvalet, D., Keefe, D., Shi, L., and Lieberman, J. (2006). Granzyme A, which causes single-stranded DNA damage, targets the double-strand break repair protein Ku70. EMBO Rep. *7*, 431–437.